Fiber-Optic Code Division Add–Drop Multiplexers

Jingshown Wu, *Senior Member, IEEE,* and Che-Li Lin

***Abstract*—In this paper, we propose a new fiber-optic code division add–drop multiplexer (ADM) which not only possesses the inherent advantages of the fiber-optic code division multiple access (CDMA), but also is fully reconfigurable. Because incoherent optical signal processing is unipolar, the dropping process is accomplished by adding the inversion of the received code. The proposed ADM is applicable to both the bus and the ring topologies. The corresponding system performance is calculated with the consideration of thermal noise, shot noise, and the amplified spontaneous emission (ASE) noise of the optical amplifier. Many interesting and useful conclusions such as the suboptimum value of various system parameters are presented.**

***Index Terms*—Add–drop multiplex (ADM), code division multiaccess (CDMA), optical fiber communication.**

I. Introduction

THE code-division multiple-access (CDMA) technology, which is conventionally used in satellite and mobile radio communications, has been applied to fiber-optic networks to provide an efficient asynchronous multiple access environment [1]–[7]. For a network to support a large number of simultaneous users, not only the size of the code set but also the autocorrelation and cross correlation properties of the spreading codes are very important. Because the intensity modulation–direct detection (IM–DD) scheme is unipolar, conventional bipolar codes used in wireless communication, such as Gold codes and maximal-length codes, are not suitable here. Therefore, systems using prime sequence codes or optical orthogonal codes have been proposed [1]–[4]. However, since they are interference limited systems, the number of simultaneous users is much less than the number of subscribers. To support a certain number of simultaneous users, the spreading sequence must be very lengthy, which makes the system hard to be realized. Therefore, error control coding and many refined system configurations have been presented [5]–[7]. In addition, two dimensional codes and the spectral coding technique have been proposed to reduce the interference penalty [8]–[13]. Recently, the CodeStream Technology Corporation has put a lot of efforts to commercialize the optical CDMA technology.[1]

For ring and bus network topologies, ADM is a very important network element. ADM can add new data channels into the network and drop the destination data channels simultaneously. For example, wavelength add–drop multiplexers (WADM's) have been widely used in wavelength division multiplexed (WDM) network [14]–[16]. The maximum number of ADM's in a network is limited by the crosstalk of WDM components and the ASE noise of cascaded optical amplifiers.

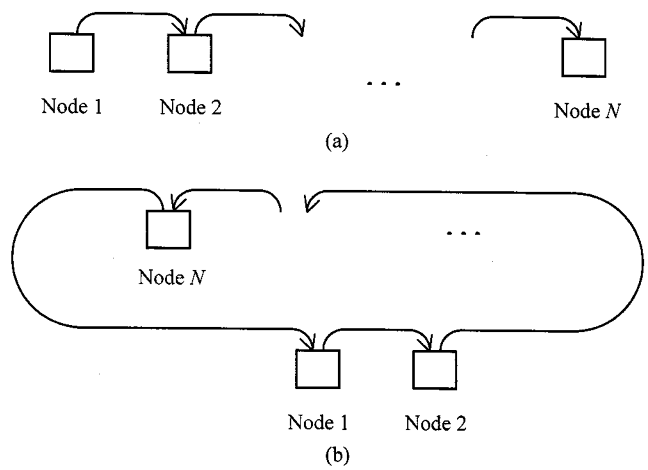

Fig. 1. Network topologies. (a) Bus topology. (b) Ring topology.

In this paper, we propose a new ADM architecture for spectrally encoded fiber-optic CDMA systems. Instead of time domain encoding, a spectrally encoded system is chosen because it does not require long spreading sequences. Besides having the inherent advantages of fiber-optic CDMA, the proposed ADM is fully reconfigurable. It is possible for a node to add or drop more than one coded channel simultaneously. It is also possible that in a multicast connection, a node does not drop the received data channel completely because other downstream nodes also need to receive that channel. The dropping process is accomplished by adding the inversion of the received code. We apply the proposed ADM in both bus and ring topologies and calculate the system performance with the consideration of thermal noise, shot noise, and the ASE noise of the optical amplifier. Many conclusions which are useful for designing the system are drawn from the numerical results.

The remainder of this paper is organized as follows. In Section II, the architecture of the proposed ADM is described. The system performance analysis for both the bus and the ring topologies is given in Section III. Section IV presents the numerical results and some discussions. Finally, Section V concludes this paper.

II. System Architectures

The two network topologies investigated in the paper are bus and ring types, which are illustrated in Fig. 1(a) and (b), respectively. We assume that there are N nodes in both network topologies. Each node is a proposed fiber-optic code division

Manuscript received May 17, 1999; revised March 9, 2000. This work was supported in part by the National Science Council, R.O.C., under Grant NSC 88-2215-E-002-035.

The authors are with the Department of Electrical Engineering, National Taiwan University, Taipei, Taiwan 106, R.O.C.

Publisher Item Identifier S 0733-8724(00)05072-6.

[1]The home page of CodeStream Tecnology Corporation: http://www.ocdma.com.

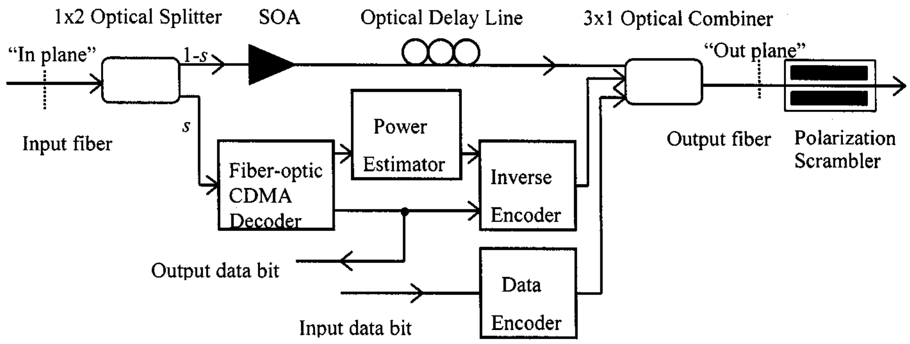

Fig. 2. The block diagrams of the proposed fiber-optic code division ADM.

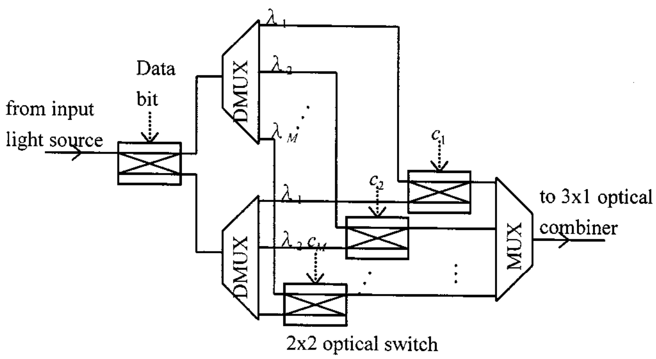

Fig. 3. The block diagrams of the data encoder.

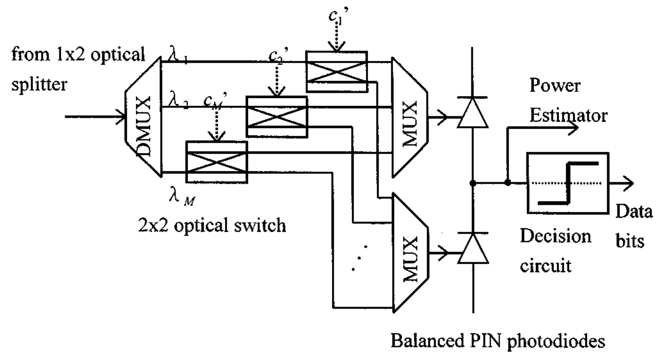

Fig. 4. The block diagrams of the fiber-optic CDMA decoder.

ADM, as shown in Fig. 2. A polarization scrambler is added at the input port of each node to depolarized the optical field [18]. The 1×2 optical splitter divides the input optical signal into two branches. The upper branch has an optical amplifier and an optical delay line. The lower branch has a fiber-optic CDMA decoder, a power estimator, and an inverse encoder. The fiber-optic CDMA decoder decodes the received data bits and sends the decoding result to the inverse encoder, which combines the information provided by the power estimator with the decoded data bits to obtain the inverse optical code patterns. The input data bits are transmitted via the the data encoder. The output of the optical delay line, that of the inverse encoder, and that of the data encoder are finally combined by a 3×1 optical combiner to form the output of the node.

The data encoder, as shown in Fig. 3, is a balanced differential optical transmitter for spectrally encoded optical CDMA systems [13]. The light source at the front of the 2×2 optical switch is a broadband superluminescent diode. The input data bit controls the state of the optical switch and thus directs the path of input light wave to either the upper or the lower wavelength-division demultiplexers (DMUX). Then M 2×2 optical switches determine the code patterns by controlling the transmission of individual wavelength component. When c_i is 0 (or 1), the ith switch is in the BAR (or CROSS) state and the wavelength λ_i from the upper (or lower) DMUX is transmitted. Finally, a wavelength-division multiplexer (MUX) is used to multiplex M wavelength channels into one output fiber.

The fiber-optic CDMA decoder is shown in Fig. 4 [13]. A DMUX is connected after the input port to demultiplex the input optical signal into M wavelength channels. When c'_i is 0 (or 1), the ith switch is in the BAR (or CROSS) state and the wavelength λ_i goes to the upper (or lower) MUX. A pair of balanced p-i-n photodiodes is placed after the MUX's to convert the optical signal into the electrical current. The output current of the balanced photodiodes is sent to both the power estimator and the decision circuit for decoding. In this paper, we assume the state vectors $\boldsymbol{c} = \{c_1, c_2, \ldots, c_M\}$ and $\boldsymbol{c} = \{c'_1, c'_2, \ldots, c'_M\}$ are from $M - 1$ row vectors of an $M \times M$ Hadamard matrix. The all "1's" row vector of Hadamard matrix is not used because of its lack of coding capability. Due to the properties of Hadamard matrix, if $\boldsymbol{c} = \boldsymbol{c}'$, the average value of the electrical current is either $M/2$ or $-M/2$ units depending on the transmitted bit. When $\boldsymbol{c} \neq \boldsymbol{c}'$, the average value of the electrical current is zero and there is no interference.

There are only three differences between the inverse encoder and the data encoder. First, in the inverse encoder, the input data bits are the complement of the received data bits. Second, the state vector in the inverse encoder is the same as that in fiber-optic CDMA decoder. Third, the purpose of the power estimator is to provide the inverse encoder the estimated optical power level of the received codes. Therefore, after the 3×1 optical combiner in the proposed node structure, the optical code pattern sent by the inverse encoder will be combined with the optical code pattern in the optical delay line. Under correct bit decoding and power estimation, the combined code pattern incurs no bit pattern when it is decoded once again by the same state vector $\boldsymbol{c}'$.

III. System Performance Analysis

In the proposed node structure, it is possible that in a multicast connection, a node does not use its inverse encoder to cancel the received code because other downstream nodes also need to receive the same data. For simplicity, it is assumed in the following analysis that a node can add and receive one coded channel at a time. After a node receives a coded channel, it drops that channel by its inverse encoder. For the multicast, the analysis is similar.

A. Bus Topology

In this subsection, we investigate the bit error probability performance of the bus topology as shown in Fig. 1(a). It is assumed that each fiber link connected between two nodes is equal in length and incurs the attenuation of L_f dB. In Fig. 2, the power gain of each node from its "In plane" to "Out plane" is r, which is stated more clearly in the following equation.

$$S_{\rm out} = S_{\rm in} \cdot r + C_{I.E.} + C_{D.E.} \tag{1}$$

where $S_{\rm in}$ and $S_{\rm out}$ are optical powers at the "In plane" and "Out plane" of a node, respectively. $C_{I.E.}$ and $C_{D.E.}$ are the optical powers transmitted from the inverse encoder and the data encoder in a node, respectively. The coupling ratio of the 1×2 optical splitter is s, i.e., the optical power of $(1-s)S_{\rm in}$ enters the upper branch of an ADM and the optical power of $s \cdot S_{\rm in}$ enters the lower branch. The optical amplifier used in each node is a traveling-wave semiconductor optical amplifier (SOA). The gain of it is expressed as follows:

$$G_{\rm SOA} = \frac{r}{1-s}. \tag{2}$$

The ASE noise induced by each SOA is $P_{\rm sp}$.

$$P_{\rm sp} = n_{\rm sp}(G_{\rm SOA} - 1)h\nu B_o \tag{3}$$

where the spontaneous emission factor, $n_{\rm sp}$, a measure of the carrier inversion, is defined as [17]

$$n_{\rm sp} = \frac{N_2}{N_2 - N_1} \tag{4}$$

and the carrier populations in the lower energy level and the exited energy level are N_1 and N_2, respectively. $h\nu$ is the photon energy and B_o is the bandwidth of the optical filter placed after the SOA. We let

$$B_o = M \cdot \Delta\nu_{ch} \tag{5}$$

where M is the number of wavelength channels in the spectrally encoded optical CDMA systems and $\Delta\nu_{ch}$ is the bandwidth of a wavelength channel.

Here, we calculate the worst case system performance, which happens when Node 1 sends data to Node N. The signal-to-noise ratio (SNR) after the balanced p-i-n photodiodes in fiber-optic CDMA decoder in Node N can be expressed as follows:

$$\text{SNR} = \frac{i_s^2}{\sigma_{\rm th}^2 + \sigma_{\rm sh}^2 + \sigma_{\rm sig-sp}^2 + \sigma_{\rm sp-sp}^2} \tag{6}$$

where i_s is electrical current due to the signal sent by Node 1

$$i_s = \frac{M}{2} sRP_s l_f^{N-1} r^{N-2} \tag{7}$$

where

- R responsivity of the p-i-n photodiode;
- P_s optical signal power of a single wavelength channel at the "Out Plane" in Node 1;
- l_f equals $10^{-L_f/10}$.

The variance of the thermal noise $\sigma_{\rm th}^2$ is

$$\sigma_{th}^2 = 2\,\frac{4k_B T}{R_L}\,\Delta f F_n \tag{8}$$

where

- k_B Boltzmann constant;
- T absolute temperature;
- R_L load resistor;
- Δf effective noise bandwidth;
- F_n accounts for the noise figure of the preamplifier.

The variance of the shot noise, σ_{sh}^2, can be expressed as

$$\sigma_{\rm sh}^2 = 2qsR\left(P_{\rm sig}^{\rm max} + P_{\rm sp}^{\rm tot}\right)\Delta f \tag{9}$$

where q is an electron charge and $P_{\rm sig}^{\rm max}$ is the maximum possible signal component received at Node N, that is the case when both the data encoder and the inverse encoder of all nodes operate simultaneously. It is also assumed that each node sends the same amount of optical power, that is, P_s per coded wavelength channel, regardless of the destination node. Therefore, we have

$$P_{\rm sig}^{\rm max} = M \sum_{i=2}^{N} l_f^{i-1} r^{i-2} P_s \tag{10}$$

$P_{\rm sp}^{\rm tot}$ is the total ASE noise contributed by the SOA's along the bus.

$$P_{\rm sp}^{\rm tot} = n_{\rm sp}(G_{\rm SOA} - 1)h\nu B_o \sum_{i=2}^{N-1} l_f^{i-1} r^{i-2} \tag{11}$$

The variance of signal–spontaneous beat noise can be expressed as

$$\sigma_{\rm sig-sp}^2 = 8R^2\left(\frac{P_{\rm sig}^{\rm max}}{2}\,\frac{P_{\rm sp}^{\rm tot}M}{B_o 2}\right)\Delta f \tag{12}$$

Then the variance of spontaneous–spontaneous beat noise is expressed as follows:

$$\sigma_{\rm sp-sp}^2 = 2R^2\left(\frac{P_{\rm sp}^{\rm tot}M}{B_o 2}\right)^2 \frac{B_o}{M}\,\Delta f. \tag{13}$$

Finally, the worst case bit error probability is shown as

$$P_b = \frac{1}{2}\,\text{erfc}\left(\sqrt{\frac{\text{SNR}}{2}}\right) \tag{14}$$

where $\text{erfc}(\cdot)$ stands for the complementary error function, defined as

$$\text{erfc}(x) = \frac{2}{\sqrt{\pi}} \int_x^{\infty} \exp(-t^2)\,dt. \tag{15}$$

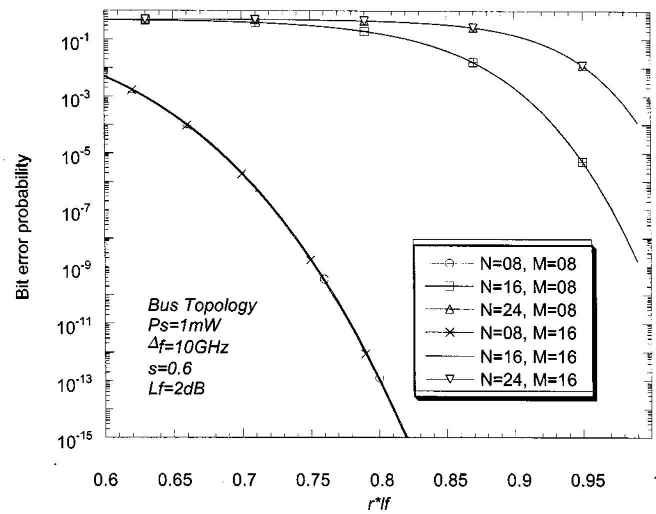

Fig. 5. Bit error probability versus $r \cdot l_f$ for the bus topology.

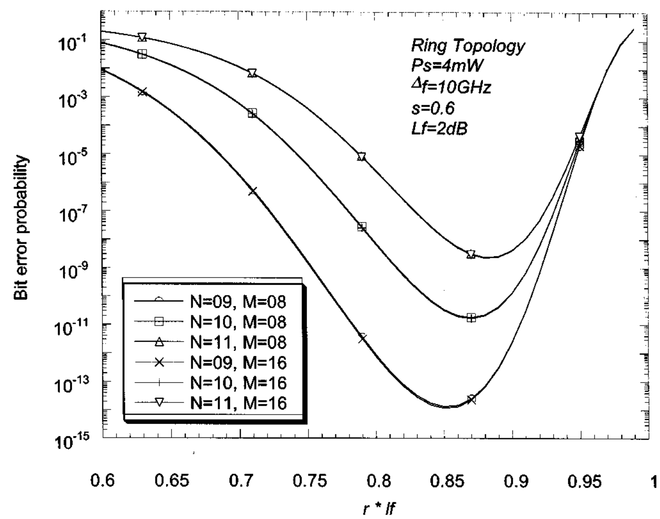

Fig. 6. Bit error probability versus $r \cdot l_f$ for the ring topology.

B. Ring Topology

In this section, we discuss the difference between ring and bus topologies. In the ring topology, the circulation of signal and noise should be taken into consideration. The worst case also happens when Node 1 sends data to Node N while the data encoder and the inverse encoder of all other nodes operate simultaneously. The SNR after the balanced PIN photodiodes in the fiber-optic CDMA decoder of Node N is expressed as follows:

$$\mathrm{SNR} = \frac{i_s^2}{\sigma_{\mathrm{th}}^2 + \sigma_{\mathrm{sh}}^2 + \sigma_{\mathrm{sig-sp}}^2 + \sigma_{\mathrm{sp-sp}}^2 + \sigma_{\mathrm{ac}}^2} \tag{16}$$

where σ_{ac}^2 is the power estimation error. The optical signal transmitted by a node will circulate back. The amount of this circulating signal power $P_{\mathrm{sig}}^{N,N}$ is given by

$$P_{\mathrm{sig}}^{N,N} = \frac{M}{2} \sum_{i=1}^{\infty} 2P_s r^{N-1} l_f^N \left(r^N l_f^N\right)^{i-1}. \tag{17}$$

In the above equation, the factor 2 before P_s accounts for the power transmitted by the inverse encoder of some node. Similarly, the amount of optical power transmitted by Node i and received by Node N $P_{\mathrm{sig}}^{i,N}$ is given by

$$P_{\mathrm{sig}}^{i,N} = P_{\mathrm{sig}}^{N,N}/(rl_f)^i \tag{18}$$

for $i = 1, 2, \ldots, N-1$. Then $P_{\mathrm{sig}}^{\max}$ should be modified as

$$P_{\mathrm{sig}}^{\max} = \sum_{i=1}^{N} P_{\mathrm{sig}}^{i,N} \tag{19}$$

The amount of ASE noise generated by the SOA in a node and received by the same node $P_{\mathrm{sp}}^{N,N}$ can be expressed by

$$P_{\mathrm{sp}}^{N,N} = n_{\mathrm{sp}}(G_{\mathrm{SOA}} - 1)h\nu B_o \sum_{i=1}^{\infty} r^{N-1} l_f^N \left(r^N l_f^N\right)^{i-1} \tag{20}$$

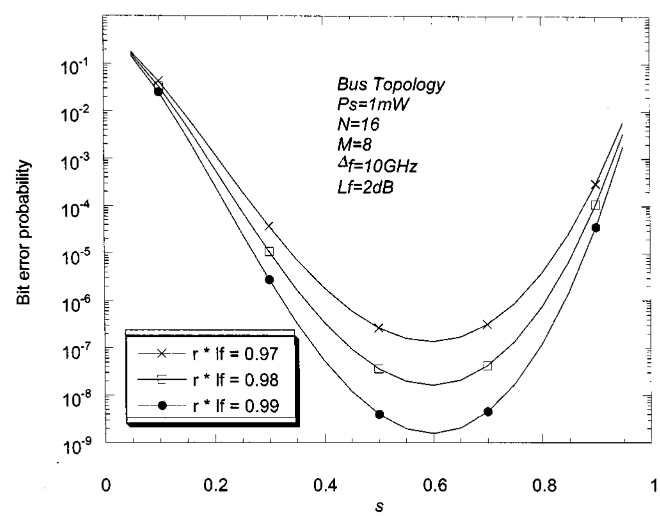

Fig. 7. Bit error probability versus s for the bus topology.

Similarly, the amount of ASE noise generated by the SOA in Node i and received by Node N, $P_{\mathrm{sp}}^{i,N}$, is

$$P_{\mathrm{sp}}^{i,N} = P_{\mathrm{sp}}^{N,N}/(rl_f)^i \tag{21}$$

for $i = 1, 2, \ldots, N-1$. Then $P_{\mathrm{sp}}^{\mathrm{tot}}$ should be modified as

$$P_{\mathrm{sp}}^{\mathrm{tot}} = \sum_{i=1}^{N} P_{\mathrm{sp}}^{i,N} \tag{22}$$

When there is power estimation error, the inverse encoder is not able to cancel the code completely. Because of the orthogonality of the Hadamard codes, the estimation error, however, affects only the nodes that receive data using the same code. Here we assume that no other node receives data using the same code as Node N. The power estimation error σ_{ac}^2 is

$$\sigma_{\mathrm{ac}}^2 = \left(\sigma_{\mathrm{th}}^2 + \sigma_{sh}^2 + \sigma_{\mathrm{sig-sp}}^2 + \sigma_{\mathrm{sp-sp}}^2\right) \sum_{i=1}^{\infty} (r^{2N} l_f^{2N})^i. \tag{23}$$

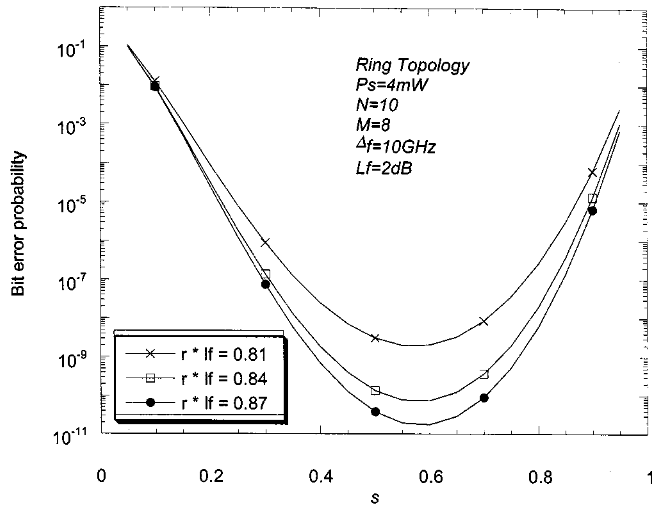

Fig. 8. Bit error probability versus s for the ring topology.

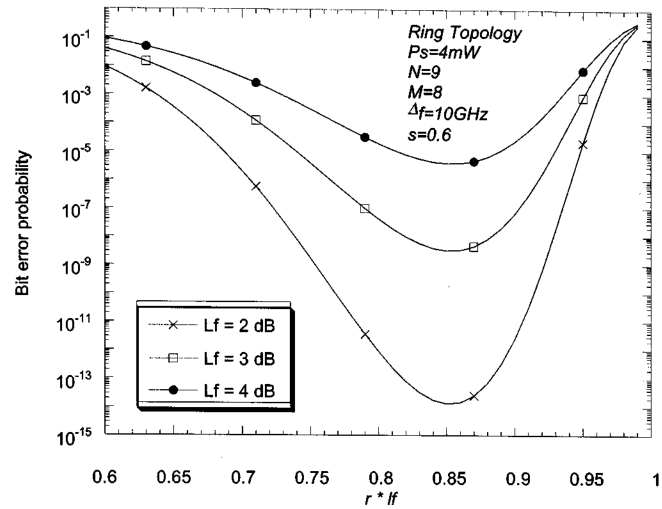

Fig. 10. Bit error probability versus $r \cdot l_f$ for the ring topology for different values of L_f.

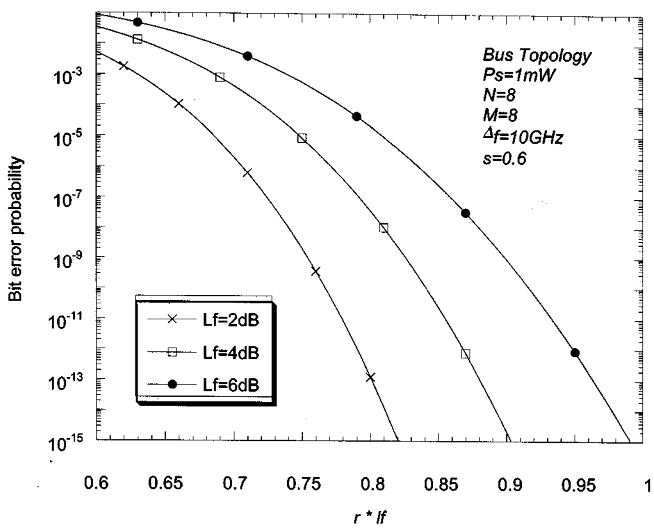

Fig. 9. Bit error probability versus $r \cdot l_f$ for the bus topology for different values of L_f.

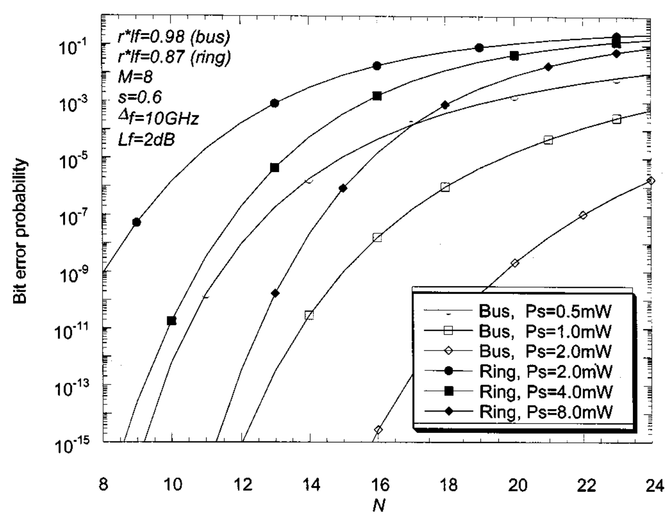

Fig. 11. Bit error probability versus N for both the bus and the ring topologies.

IV. Numerical Examples and Discussions

The numerical examples of the bit error probability analysis are given in this section. The setting of some parameters are as follows: $R_L = 1000\,\Omega$, $F_n = 3$ dB, $T = 300$K, $\Delta f = 10$ GHz, $R = 0.8$ A/W, $n_{\rm sp} = 1.4$, and $\Delta\nu_{ch} = 0.8$ nm. The center of wavelength channels is at 1.55 μm. Fig. 5 shows the bit error probability versus the total loss of a node and a fiber link, $r \cdot l_f$, for the bus topology. It is seen that the larger $r \cdot l_f$ is , the smaller bit error probability we obtain. When the number of nodes in the network, N, increases, the performance degrades significantly. The number of wavelength channels in the spectrally encoded optical CDMA systems, M, however, has little effect on the system performance. The bit error probability versus $r \cdot l_f$ for the ring topology, as shown in Fig. 6, is very different from that for the bus topology. The value of $r \cdot l_f$ which possesses the smallest bit error probability is around 0.87. When the value of $r \cdot l_f$ gets close to one, the lasing effect in the ring topology corrupts the system performance.

Figs. 7 and 8 show the bit error probability versus s for the two network topologies. It is seen that the the optimal values of s are around 0.6. If s is too close to zero, the optical power for the fiber-optic CDMA decoder will be too small. On the other hand, if s is close to one, the SOA needs to provide higher gain, thus inducing larger ASE noise. Figs. 9 and 10 show the bit error probability versus $r \cdot l_f$ for different values of L_f. It is also true that to compensate larger fiber link loss, the SOA has to provide higher gain. Therefore, the larger L_f is, the worse the system performance we obtain. Because of the circulation effect, the ring topology is more susceptible to the value of L_f than the bus topology. Finally, Fig. 11 gives the relation between bit error probability and N for both the bus and ring topologies. We see that the required P_s in the ring topology is higher than that in the bus topology. Furthermore, the system performance is more sensitive to N in the ring topology than in the bus topology.

V. Conclusion

In this paper, a fully reconfigurable fiber-optic code division add–drop multiplexer (ADM) is proposed. Among many fiber-optic CDMA technologies, spectrally encoded system is used because when combined with Hadamard codes, it provides an orthogonal sequence set and does not require long spreading sequences. We apply the proposed ADM in both the bus and the ring topologies and calculate the system performance with the consideration of thermal noise, shot noise, and the ASE noise of the optical amplifier. From the above analysis, it is seen that because the system performance for both topologies is dominated by the ASE noise, the number of nodes and the link loss have pronounced effect on the bit error probability. We also know that besides determining the number of available codes, the number of wavelengths has little effect on the bit error performance. The performance of the ring topology is much worse than that of the bus topology because of the circulation effect in the ring network. However, if full connectivity is desired in the bus topology, there must be another bus transmitting data in the opposite direction.

References

[1] P. R. Prucnal, M. A. Santoro, and T. R. Fan, "Spread spectrum fiber-optic local area network using optical processing," *J. Lightwave Technol.*, vol. LT-4, pp. 547–554, May 1986.

[2] W. C. Kwong, P. A. Perrier, and P. R. Prucnal, "Performance comparison of asynchronous and synchronous code-division multiple-access techniques for fiber-optic local area networks," *IEEE Trans. Commun.*, vol. 39, pp. 1625–1634, Nov. 1991.

[3] J. A. Salehi, "Code division multiple-access techniques in optical fiber networks—Part I: Fundamental principles," *IEEE Trans. Commun.*, vol. 37, pp. 824–833, Aug. 1989.

[4] J. A. Salehi and C. A. Brackett, "Code division multiple-access techniques in optical fiber networks—Part II: Systems performance analysis," *IEEE Trans. Commun.*, vol. 37, pp. 834–842, Aug. 1989.

[5] J.-H. Wu and J. Wu, "Synchronous fiber-optic CDMA using hard-limiter and BCH codes," *J. Lightwave Technol.*, vol. LT-13, pp. 1169–1176, June 1995.

[6] T. Ohtsuki, "Channel interference cancellation using electrooptic switch and optical hardlimiters for direct-detection optical CDMA systems," *J. Lightwave Technol.*, vol. 16, pp. 520–526, Apr. 1998.

[7] C.-L. Lin and J. Wu, "A synchronous fiber-optic CDMA system using adaptive optical hardlimiter," *J. Lightwave Technol.*, vol. 16, pp. 1393–1403, Aug. 1998.

[8] E. Park, A. J. Mendez, and E. M. Garmire, "Temporal/spatial optical CDMA networks-design, demonstration, and comparison with temporal networks," *IEEE Photon. Technol. Lett.*, vol. 4, pp. 1160–1162, Oct. 1992.

[9] A. J. Mendez, J. L. Lambert, J.-M. Morookian, and R. M. Gagliardi, "Synthesis and demonstration of high speed, bandwidth efficient optical code division multiple access tested at 1 Gb/s throughput," *IEEE Photon. Technol. Lett.*, vol. 6, pp. 1146–1149, Sept. 1994.

[10] D. Zaccarin and M. Kavehrad, "An optical CDMA system based on spectral encoding of LED," *IEEE Photon. Technol. Lett.*, vol. 5, pp. 479–482, Apr. 1993.

[11] L. Nguyen, B. Aazhang, and J. F. Young, "All-optical CDMA with bipolar codes," *Electron. Lett.*, vol. 31, no. 6, pp. 469–470, Mar. 1995.

[12] C.-C. Chang, H. P. Sardesai, and A. M. Weiner, "Code-division multiple-access encoding and decoding of femtosecond optical pulses over a 2.5-km fiber link," *IEEE Photon. Technol. Lett.*, vol. 10, pp. 171–173, Jan. 1998.

[13] C. F. Lam, D. T. K. Tong, M. C. Wu, and E. Yablonovitch, "Experimental demonstration of bipolar optical CDMA system using a balanced transmitter and complementary spectral encoding," *IEEE Photon. Technol. Lett.*, vol. 10, pp. 1504–1506, Oct. 1998.

[14] K. Oda and H. Toba, "An optical FDM-add/drop multiplexing ring network utilizing fiber Fabry–Perot filters and optical circulators," *IEEE Photon. Technol. Lett.*, vol. 5, pp. 825–828, July 1993.

[15] W. D. Zhong, S. Dods, J. P. R. Lacey, and R. S. Tucker, "Reconfigurable multichannel add-drop multiplexer with improved performance," *Electron. Lett.*, vol. 32, no. 16, pp. 1477–1478, Aug. 1996.

[16] B. S. Johansson, C. R. Batchellor, and L. Egnell, "Flexible bus: A self-restoring optical ADM ring architecture," *Electron. Lett.*, vol. 32, no. 25, pp. 2338–2339, Dec. 1996.

[17] N. A. Olsson, "Lightwave systems with optical amplifiers," *J. Lightwave Technol.*, vol. 7, pp. 1071–1082, July 1989.

[18] F. Heismann, "Compact electro-optic polarization scramblers for optially amplified lightwave systems," *J. Lightwave Technol.*, vol. 14, pp. 1801–1814, Aug. 1996.

Jingshown Wu (S'73–M'78–SM'99) received the B.S. and M.S. degrees in electrical engineering from National Taiwan University, Taipei, Taiwan, R.O.C., and the Ph.D. degree from Cornell University, Ithaca, NY, in 1970, 1972, and 1978, respectively.

In 1978, he joined Bell Laboratories, where he worked on digital network standards and performance, and optical fiber communication systems. In 1984, he joined the Department of Electrical Engineering of National Taiwan University as Professor and was the Chairman of the Department from 1987 to 1989. He was also the Director of the Communication research Center, College of Engineering of the University from 1992 to 1995. From 1995 to 1998, he was the Director of the Division of Engineering and Applied Science Council, R.O.C., on leave from the university. Since 1999, he has been the Chairman of the Commission on Research and Development, responsible for the direction of the center for sponsor programs. He is interested in optical fiber communications, wireless communication, and computer communication networks.

Dr. Wu is a Life Member of the Chinese Institute of Engineers, the Optical Society of China, and Institute of Chinese Electrical Engineers.

Che-Li Lin was born in Taipei, Taiwan, R.O.C., in 1974. He graduated from Yeng-Ping High School, Taipei, in 1991, with the best academic performance among all graduates. He received the B.S. and Ph.D. degrees both in electrical engineering from National Taiwan University, Taipei, Taiwan, in 1995 and 1999, respectively.

Presently, he is an Engineer in Protocol Design Technology Department of Computer and Communications Research Laboratories, Industrial Technology Research Institute, Hsinchu, Taiwan. His research interests include lightwave communication systems, IMT-2000, high speed communication networks, and spread spectrum communication.